Global Change Biology

Global Change Biology (2017) **23**, 3092–3106, doi: 10.1111/gcb.13602

Gross primary production responses to warming, elevated CO_2, and irrigation: quantifying the drivers of ecosystem physiology in a semiarid grassland

EDMUND M. RYAN[1], KIONA OGLE[2,3], DREW PELTIER[3], ANTHONY P. WALKER[4], MARTIN G. DE KAUWE[5], BELINDA E. MEDLYN[6], DAVID G. WILLIAMS[7], WILLIAM PARTON[8], SHINICHI ASAO[8], BERTRAND GUENET[9], ANNA B. HARPER[10], XINGJIE LU[11], KRISTINA A. LUUS[12,†], SÖNKE ZAEHLE[12], SHIJIE SHU[13], CHRISTIAN WERNER[14], JIANYANG XIA[15,16] and ELISE PENDALL[6,7]

[1]*Lancaster Environment Centre, Lancaster, UK,* [2]*School of Informatics, Computing, and Cyber Systems, Northern Arizona University, Flagstaff, AZ, USA,* [3]*Department of Biological Sciences, Northern Arizona University, Flagstaff, AZ, USA,* [4]*Environmental Sciences Division and Climate Change Science Institute, Oak Ridge National Laboratory, Oak Ridge, TN, USA,* [5]*Department of Biological Sciences, Macquarie University, Sydney, NSW 2109, Australia,* [6]*Hawkesbury Institute for the Environment, Western Sydney University, Penrith, NSW, Australia,* [7]*Department of Botany, University of Wyoming, Laramie, WY, USA,* [8]*Natural Resource Ecology Laboratory, Colorado State University, Fort Collins, CO 80523-1499, USA,* [9]*Laboratoire des Sciences du Climat et de l'Environnement, LSCE/IPSL, CEA-CNRS-UVSQ, Université Paris-Saclay, F-91191 Gif-sur-Yvette, France,* [10]*College of Engineering, Mathematics, and Physical Sciences, University of Exeter, Exeter, UK,* [11]*CSIRO Ocean and Atmosphere, PBM #1, Aspendale, Vic. 3195, Australia,* [12]*Biogeochemical Integration Department, Max Planck Institute for Biogeochemistry, Hans-Knöll-Str. 10, 07745 Jena, Germany,* [13]*Department of Atmospheric Sciences, University of Illinois, 105 South Gregory Street, Urbana, IL 61801-3070, USA,* [14]*Senckenberg Biodiversity and Climate Research Centre (BiK-F), Senckenberganlage 25, 60325 Frankfurt, Germany,* [15]*Department of Microbiology & Plant Biology, University of Oklahoma, Norman, OK 73019, USA,* [16]*Research Center for Global Change and Ecological Forecasting, East China Normal University, Shanghai 200062, China*

Abstract

Determining whether the terrestrial biosphere will be a source or sink of carbon (C) under a future climate of elevated CO_2 (eCO_2) and warming requires accurate quantification of gross primary production (GPP), the largest flux of C in the global C cycle. We evaluated 6 years (2007–2012) of flux-derived GPP data from the Prairie Heating and CO_2 Enrichment (PHACE) experiment, situated in a grassland in Wyoming, USA. The GPP data were used to calibrate a light response model whose basic formulation has been successfully used in a variety of ecosystems. The model was extended by modeling maximum photosynthetic rate (A_{max}) and light-use efficiency (Q) as functions of soil water, air temperature, vapor pressure deficit, vegetation greenness, and nitrogen at current and antecedent (past) timescales. The model fits the observed GPP well (R^2 = 0.79), which was confirmed by other model performance checks that compared different variants of the model (e.g. with and without antecedent effects). Stimulation of cumulative 6-year GPP by warming (29%, P = 0.02) and eCO_2 (26%, P = 0.07) was primarily driven by enhanced C uptake during spring (129%, P = 0.001) and fall (124%, P = 0.001), respectively, which was consistent across years. Antecedent air temperature ($Tair_{ant}$) and vapor pressure deficit (VPD_{ant}) effects on A_{max} (over the past 3–4 days and 1–3 days, respectively) were the most significant predictors of temporal variability in GPP among most treatments. The importance of VPD_{ant} suggests that atmospheric drought is important for predicting GPP under current and future climate; we highlight the need for experimental studies to identify the mechanisms underlying such antecedent effects. Finally, posterior estimates of cumulative GPP under control and eCO_2 treatments were tested as a benchmark against 12 terrestrial biosphere models (TBMs). The narrow uncertainties of these data-driven GPP estimates suggest that they could be useful semi-independent data streams for validating TBMs.

Keywords: Bayesian modeling, carbon cycle, elevated CO_2, grasslands, gross primary production, multifactor global change experiment, warming

Received 28 September 2016 and accepted 8 November 2016

Correspondence: Edmund M. Ryan, Lancaster Environment Centre, Bailrigg, Lancaster LA1 4YW, UK, tel. +44 (0) 1524 594009, fax +44 (0)1524 61536, e-mail: edmund.ryan@lancaster.ac.uk

[†]Present address: Dublin Institute of Technology, Dublin D02 TD3, Ireland

Introduction

Gross primary production (GPP) is the largest flux in the global carbon (C) cycle, representing the gross amount of C removed from the atmosphere by plants via photosynthesis at the ecosystem scale (Chapin *et al*., 2006). GPP represents the input of C into the terrestrial biosphere, which plays an important role in determining the magnitudes of the flows and stores of C within plants and soil (Williams *et al*., 2005; Beer *et al*., 2010). Despite its importance, there remains large uncertainty in global model projections of future GPP – both globally and regionally – under anticipated future levels of CO_2 and warming (Arora *et al*., 2013; Richardson *et al*., 2013), and there is an urgent need to determine the causes of these uncertainties (Friedlingstein *et al*., 2014). Improved accuracy of these model predictions is critical in determining whether the terrestrial biosphere is likely to be a future sink or source of C.

While the responses of net primary production (NPP) to elevated CO_2 (eCO_2) are well studied, less work has directly evaluated GPP, partly because it is not directly measurable. The few studies that exist on the singular effect of eCO_2 on GPP report a positive effect. For example, Wittig *et al.* (2005) found a ~80% stimulation of GPP for *Populus* trees growing under eCO_2 over a 3-year period. Likewise, using 3 years of leaf-level photosynthesis data, Luo *et al.* (2001) found a ~40% increase in modeled GPP under eCO_2. A stimulation of NPP under eCO_2 suggests a stimulation of GPP if it is assumed that NPP is proportional to GPP (Waring *et al*., 1998; Williams *et al*., 2005). A ~20% increase in NPP under eCO_2 is expected in mid-latitudes (Luo *et al*., 2006), and this should translate into increased GPP. However, semiarid grasslands exhibit large variation in NPP responses to eCO_2 (0–100%), which is primarily driven by spatial and temporal precipitation variability (Polley *et al*., 2013). The stimulation of NPP by eCO_2 has been shown to be suppressed if the ecosystem is nitrogen limited (Norby & Zak, 2011). GPP should also be affected by responses of leaf-level photosynthesis at light saturation (A_{sat}), which increases with eCO_2 in trees (~45%), grasses (~35%), shrubs (~20%), and crops (~35%) (Ainsworth & Long, 2005), but scaling from leaf-level A_{sat} to ecosystem-level GPP is fraught with uncertainties (Arp, 1991; McLeod & Long, 1999; Morgan *et al*., 2001).

Warming affects GPP directly through the effect of temperature on leaf photosynthesis, and indirectly via alterations in nitrogen mineralization and water availability (Cox *et al*., 2000; Ciais *et al*., 2014). As with eCO_2, a stimulation of NPP under warming suggests a stimulation of GPP if it is assumed that NPP is proportional to GPP (Waring *et al*., 1998; Williams *et al*., 2005). Terrestrial biosphere models (TBMs) predict a reduction in NPP with long-term warming; if warming reaches 3–5 °C by 2100 under a high CO_2 emissions scenario (Collins *et al*., 2013), global terrestrial NPP may decrease by 15–100% (10–60 PgC yr^{-1}) (Roy *et al*., 2001; Friedlingstein *et al*., 2006; Sitch *et al*., 2008). Retrospective analyses also show a negative effect of warming on NPP, such as a ~9% decrease in global NPP between 1980 and 2002, which offset the CO_2 fertilization effect (Magnani *et al*., 2007). However, the magnitude of the GPP and NPP responses to warming varies among biomes, with northern latitudes expected to exhibit the largest increases (Landsberg & Waring, 1997; Piao *et al*., 2008; Rustad, 2008). At the site level, a meta-analysis of 32 separate warming experiments found a positive effect of warming on NPP for tundra sites, but no effect for temperate forest and grassland sites (Rustad *et al*., 2001). At the regional level, a surface temperature increase of 2 °C between 1988 and 2008 in northern latitudes stimulated GPP during the spring and fall (Landsberg & Waring, 1997; Piao *et al*., 2008; Rustad, 2008).

TBMs assume that the interactive effect of eCO_2 and warming is positive (Norby & Luo, 2004; Luo *et al*., 2008). Field data from climate change experiments support this for certain years (Dukes *et al*., 2005), but over multiple years there is growing evidence that the positive interactive response does not exist or is not as strong as models suggest (Shaw *et al*., 2002; Dieleman *et al*., 2012). The effects of eCO_2 and warming – whether singular or combined – may be dependent upon precipitation inputs in water-limited ecosystems (Knapp & Smith, 2001; Fay *et al*., 2003; Huxman *et al*., 2004; Schwinning *et al*., 2004). For example, an experiment in a mixed C3/C4 semiarid grassland found that aboveground NPP was increased by ~80% when annual precipitation was delivered in a few, large rain events compared with more frequent, smaller events (Heisler-White *et al*., 2008). Recent work has generalized this by considering the effect of past or antecedent conditions on primary production. For example, Ogle *et al.* (2015) found that event size and antecedent precipitation explained 75% of the variation in aboveground NPP (ANPP) in the same semiarid grassland. Likewise, antecedent soil water content was a significant predictor of ANPP in a tall grass prairie (Sherry *et al*., 2008).

We identified three major knowledge gaps with regard to the response of GPP to climate change. First, few climate change experiments have investigated the combined effects of eCO_2 and warming on primary production (Luo *et al*., 2008). Second, most of the literature on the ecosystem responses of primary productivity to eCO_2 and warming are based on measurements of NPP (as highlighted above); very few evaluate GPP,

yet this is critical for constraining predictions of C cycle responses to climate change (Norby & Luo, 2004). Third, while analyses of climate change experiments often report that treatment effects are contingent upon background climate conditions (e.g., Morgan *et al*., 2011), the effects of antecedent climate conditions are often not evaluated.

To address these knowledge gaps, we measured and analyzed GPP for 6 years as part of the Prairie Heating and CO_2 Enrichment (PHACE) Experiment. The experiment consisted of six treatments, four of which were applied in a full factorial design with CO_2 (ambient vs. elevated) and temperature (ambient vs. warming), and two others involved deep and shallow irrigation applied under ambient CO_2 and temperature. We drew upon this 6-year dataset to address three questions: (i) How does GPP respond to the main and interactive effects of eCO_2 and warming in the context of variable precipitation? (ii) What environmental and meteorological factors (e.g., soil water content, antecedent conditions) govern potential responses of GPP to climate change? Finally, we illustrate how our modeling approach can be applied to generate more realistic data products for informing TBMs, and we ask: (iii) How does the inclusion of antecedent conditions affect the magnitude and uncertainty in such GPP data products? Accurate estimation of uncertainty is essential in model evaluation exercises, and we provide a full accounting of uncertainty in our analyses.

Materials and methods

Site description

The PHACE site is situated near Cheyenne, Wyoming at an elevation of 1930 m, with a semiarid, temperate climate. Thirty-year mean annual temperature is 8.3 °C and precipitation is 378 mm, with ~75% falling during the growing season (Zelikova *et al*., 2015). The vegetation is a mixed-grass prairie, dominated by two C3 grasses, western wheatgrass (*Pascopyrum smithii* (*Rydb.*) *A. Löve*) and needle-and-thread grass (*Hesperostipa comata Trin and Rupr*), and the C_4 perennial grass blue grama (*Bouteloua gracilis* (*H.B.K.*) *Lag*). Live plant cover ranges up to 70% of ground area (Zelikova *et al*., 2015), and roots extend to 40 cm with 75% of root biomass occurring above 15 cm depth (Carrillo *et al*., 2014). The soil is a fine-loamy, mixed, mesic Aridic Argiustolls, and biological crusts are not present (Bachman *et al*., 2010).

Experimental design

The PHACE experiment was set up as an incomplete factorial design consisting of six treatments and five replicate plots (3.4 m in diameter) per treatments (Morgan *et al*., 2011). Four of the six treatments – abbreviated as ct, cT, Ct, CT – are a full factorial design of atmospheric CO_2 (ambient at 380–400 ppm [abbreviated as 'c'] versus elevated at 600 ppm ['C']) and warming (no warming ['t'] versus heated by 1.5 °C in the daytime and 3.0 °C in the nighttime ['T']). The increase in atmospheric CO_2 (600 ppm) for the elevated CO_2 plots (Ct and CT) was achieved using Free Air CO_2 Enrichment (FACE) technology (Miglietta *et al*., 2001). Warming was simulated (cT and CT) by applying a ceramic heater system using a proportional–integral–derivative (PID) feedback loop (Kimball, 2005).

The final two treatments (cts and ctd) involve irrigation applied to ambient CO_2 and no warming plots (shallow ['s'] or deep ['d'] irrigation). In the context of the PHACE study, the main aim of the irrigation treatments was to test the hypothesis that responses to eCO_2 are indirectly due to increases in soil water. As such, water was applied to the cts and ctd plots in an effort to increase their soil water contents to match that of the Ct treatment. In the cts treatment, irrigation was applied when soil moisture fell below 85% of Ct at the 5–25 cm depth: In 2007, five 18-mm precipitation events were applied (totaling 90 mm); during 2008–2011, three 21-mm events per year were applied (totaling 63 mm each year), and in 2012, four 65-mm events (totaling 260 mm) were applied. The total amount of water applied to the ctd plots was the same as the cts plots, but water was only added twice per year (spring and fall), in approximately equal amounts.

Data description

All data were measured in the field from 2007 to 2012, and consisted of GPP (μmol C m^{-2} s^{-1}), associated air temperature (Tair; °C), volumetric soil water content (SWC; m^2/m^2), ecosystem phenology ('greenness'; %), photosynthetically active radiation (PAR; μmol quanta m^{-2} s^{-1}), aboveground plant nitrogen content (N; g m^{-2}), and relative humidity (RH; %); vapor pressure deficit (VPD; kPa) was computed from Tair and RH. GPP data were obtained indirectly as the difference between measurements of net ecosystem exchange (NEE; μmol C m^{-2} s^{-1}) and ecosystem respiration (R_{eco}; μmol C m^{-2} s^{-1}) that were made within 2 min of each other. NEE was measured using a 0.1-m^3 canopy gas exchange chamber by measuring the rate of change of CO_2 concentration for 1 min (Jasoni *et al*., 2005; Bachman *et al*., 2010). R_{eco} was measured immediately afterward and in exactly the same way as the NEE one, except that an opaque cover was placed over the chamber to eliminate light. Midday measurements were made on a total of 88 days over six growing seasons (May through September), and measurement days were typically separated by 2–4 weeks. Additional measurements of NEE and R_{eco}, and thus GPP, were made every 6 weeks at five measurement times per day in each plot (nominal times = 04:00, 09:00, 12:00, 16:00, and 21:00). More details on the methods can be found in Bachman *et al*. (2010) and Pendall *et al*. (2013). See Ryan *et al*. (2015) for descriptions of the environmental data and the gap filling employed to estimate missing covariate data on certain days and hours.

Data synthesis and modeling

We fit a nonlinear mixed-effects model to the GPP data to quantify how GPP varied among the experimental treatments at the season, annual, and multi-annual scales. The goal of this analysis is twofold: (i) to quantify the combined effects of the categorical treatment effects and the time-varying concurrent and antecedent environmental effects (addressing questions 1 and 2), and (ii) to estimate GPP on nonmeasurement times, while accounting for different sources of uncertainty, thus allowing us to gap-fill the GPP dataset and produce estimates of cumulative GPP fluxes (addressing question 3).

Given the distributional properties of the observed GPP data (GPP^{obs}), we assumed that GPP^{obs} followed a normal distribution. Thus, observation i (i = 1,. . ., 2456):

$$GPP_i^{obs} \sim \text{Normal}(\mu_i, \sigma^2_{t(i)}) \quad (1)$$

μ is the mean or predicted GPP value, σ^2 represents the observation variance, and $t(i)$ indicates treatment t (t = 1, 2, . . ., 6 treatment levels) associated with observation i. We employ a semi-empirical model for the mean GPP, μ, based on the rectangular hyperbola light-response model (Thornley, 1976; Landsberg & Waring, 1997; Falge *et al*., 2001; Desai *et al*., 2008), which we adapted to include the effect of atmospheric CO_2 concentration (Acock *et al*., 1976). We lack sufficient data to parameterize more complex or mechanistic models (E.g. Farquhar *et al*., 1980). However, the light-response or radiation-use efficiency type model has been frequently applied, in various formulations, to ecosystem-level GPP and NPP flux data (see above references), and thus, there is good precedence for using it here. The model for μ is:

$$\mu_i = \frac{Q_i \text{PAR}_i A_{\max_i} C_i}{Q_i \text{PAR}_i + A_{\max_i} C_i} \quad (2)$$

PAR_i is the measured PAR (μmol m^{-2} s^{-1}); Q_i (μmol CO_2 μmol^{-1} quanta) is the quantum yield or canopy light-use efficiency (i.e., the slope of the light response curve at PAR = 0); $A_{\max_i}$ (μmol C m^{-2} s^{-1}) is the maximum CO_2 uptake rate of the canopy (maximum GPP) at light saturation. $C_i = c_j \exp\left(CO_{2_i} - \overline{CO_{2_j}}\right)$ accounts for variation in atmospheric CO_2 relative to the mean observed atmospheric [CO_2] ($\overline{CO_{2_j}}$) in the ambient (j = 1; ct, cT, ctd, cts) and elevated (j = 2; Ct, CT) CO_2 plots, where CO_{2_i} is the measured atmospheric [CO_2], and the parameter c_j describes the effect of deviations from the mean concentration ($\overline{CO_{2_j}}$ = 376 ppm and 572 ppm for j = 1 and j = 2, respectively). An exponential function is applied to the deviations to ensure $C_i > 0$.

To capture potential temporal changes in the GPP response, we modeled Q and A_{max} as functions of various biotic (greenness and N) and abiotic (SWC, Tair, and VPD) factors at both current and antecedent (described in detail in the section below) timescales. It is well known that plant photosynthesis is partly governed by leaf N content (Williams *et al*., 1996; Landsberg & Waring, 1997; Magnani *et al*., 2007) and temperature (Farquhar *et al*., 1980; Bernacchi *et al*., 2001) via their effects on enzyme-mediated reactions. VPD also plays an important role via its effect on stomatal conductance, which in turn controls photosynthetic rates (Collatz *et al*., 1991; Medlyn *et al*., 2011). Furthermore, vegetation greenness is expected to correspond to GPP; for example, satellite estimates of GPP are inferred from the light reflectance of the vegetation, which describes greenness of the vegetation. To ensure that A_{max} is positive, we modeled A_{max} on the log scale, and to constrain Q between 0 and 1, we modeled Q on the logit scale. For example, we modeled log (A_{max}) as a linear function of the aforementioned current and antecedent (subscript = ant) biotic and abiotic drivers, with parameters that vary by treatment t (t = 1, 2, . . ., 6) associated with observation i:

$$\begin{aligned}\log(A_{\max_i}) = {} & \alpha_{0,t(i)} + \alpha_{1,t(i)}\text{SWC}_i + \alpha_{2,t(i)}\text{VPD}_i \\ & + \alpha_{3,t(i)}\text{Tair}_i + \alpha_{4,t(i)}\text{SWC}_{ant,i} + \alpha_{5,t(i)}\text{VPD}_{ant,i} \\ & + \alpha_{6,t(i)}\text{Tair}_{ant,i} + \alpha_{7,t(i)}N_i + \alpha_{8,t(i)}\text{Greenness}_i \\ & + \alpha_{9,t(i)}\Delta\text{Greenness}_{ant,i} + \text{interactions} + \epsilon_{t(i),p(t(i))}\end{aligned} \quad (3)$$

$\varepsilon_{t,p}$ represents a plot (nested in treatment) random effect, and $p(t(i))$ indicates plot p associated with treatment t and observation i (p = 1, 2, 3, 4, 5 for each treatment). $\Delta\text{Greenness}_{ant}$ represents the antecedent rate of change of greenness; when greenness is increasing, $\Delta\text{Greenness}_{ant} > 0$, and when leaves are senescing, $\Delta\text{Greenness}_{ant} < 0$. We define 'interactions' in Eqn (3) to potentially include all two-way interactions between the covariates indicated in Eqn (3). Preliminary analysis identified five-two-way interactions (of 36 possible) that were most important for understanding GPP (see Appendix S1 for details of preliminary analysis), including Tair × Tair, SWC_{ant} × Tair_{ant}, SWC_{ant} × VPD_{ant}, SWC × SWC_{ant} Tair × Tair_{ant}, and VPD × Tair; these five interactions represent the 'interactions' term and are assigned interaction effects parameters $\alpha_{10,t}$ – $\alpha_{15,t}$, respectively. Including these interactions is further justified because: (i) Tair × Tair accounts for a potential peaked temperature response; (ii) SWC_{ant} × Tair_{ant} indicates the seasonality of moisture availability; (iii) SWC_{ant} × VPD_{ant} indicates differential below- versus aboveground water stress effects; and (iv) previous studies have reported important interactions between current and antecedent factors. Regarding the last point, C fluxes are likely to respond differently to a rain event (increase in current SWC) that occurs during a dry period (low SWC_{ant}) compared with during a wet period (high SWC_{ant}) (Arp, 1991; Cable *et al*., 2013; Barron-Gafford *et al*., 2014; Ryan *et al*., 2015), thus reflecting potential hysteresis patterns (Barron-Gafford *et al*., 2011; Oikawa *et al*., 2014).

The function for logit (Q) is the same as for log (A_{max}) except that: (i) there is no N term because N is primarily expected to affect the amount of RuBisCO in the photosynthetic tissues, which in turn primarily limits A_{max} (Reich *et al*., 2009); and (ii) it has its own nested plot random effects and treatment-specific effects parameters (β_0,. . ., β_{14}) (see Table 3 for a summary of model parameters).

Quantification of antecedent drivers

We characterized and quantified antecedent covariates following the stochastic antecedent modeling (SAM) framework described by Ogle *et al.* (2015); examples of practical implementation are given by Ryan *et al.* (2015), Cable *et al.* (2013), and Barron-Gafford *et al.* (2014). Traditional methods of

defining antecedent variables often compute a deterministic average of the variable over a fixed past time period. SAM is different in that it allocates parameters ('importance weights') to specific periods in the past, thus enabling quantification of the relative importance of the variable at those different past times. Following Cable *et al*. (2013) and Ryan *et al.* (2015), we allowed GPP to be influenced by Tair and VPD over daily timescales, and by SWC and greenness over weekly timescales. In general, we describe the antecedent variable (X_{ant}) associated with observation i as:

$$X_{ant,i} = \sum_{k=1}^{N_{\text{periods}}} W_{X_{k,t(i)}} \bar{X}_{tp(i)-k+1,p(t(i))} \quad (4)$$

where X = VPD or Tair, $\bar{X}$is the 24-h mean for a particular day or time period, k is the time lag into the past (for $N_{\text{period}} = 7$ time steps) such that when $k = 1$, $\bar{X}$ is the observed 24-h mean that occurred during $tp(i)$, the time period associated with observation i; again, $t(i)$ and $p(t(i))$ are the treatment (t = 1,..,6) and plot (p = 1,..,5 per treatment) associated with observation i. W_X are the weight parameters to be estimated. The expression for SWC_{ant} is similar to Eqn (4) except that $\bar{X}$ is the 7-day mean for a particular week such that tp denotes the week associated with each observation and k denotes the time (week scale) lag ($N_{\text{periods}} = 6$); as done in Ryan *et al.* (2015), we allocated a separate weight for each of the first few weeks in the past (k = 1, 2, 3, 4), the fifth (k = 5) weight to past weeks 5–6, and the sixth (k = 6) weight to past weeks 7–10. We made a slight modification to calculate $\Delta\text{Greenness}_{\text{ant}}$:

$$\Delta\text{Greenness}_{ant,i} = \sum_{k=1}^{N_{\text{periods}}} W_{X_{k,t(i)}} \left(\bar{X}_{tp(i)-k+1,p(t(i))} - \bar{X}_{tp(i)-k,p(t(i))}\right) \quad (5)$$

where $\bar{X}$, i, k, t, tp, and p are as defined previously for the weekly scale covariates. Like SWC_{ant}, the time periods are on a weekly scale, but k = 1, 2, 3, and 4 correspond to the past week, 2 weeks ago, 3 weeks ago, and 4 weeks ago ($N_{\text{periods}} = 4$), respectively.

We refer to the model described above as the 'main' model. We also implemented an 'alternative' model that excludes all antecedent covariates from the Q and $A_{\max}$ functions, as defined in Eqn (3), to evaluate the importance of including antecedent effects. The alternative model (no antecedent effects) is more similar to the types of models that are often applied for partitioning eddy-covariance NEE data into its GPP and ecosystem respiration components, such as those described in the review paper by Desai *et al*. (2008).

Model implementation and assessment

We implemented the model within a hierarchical Bayesian framework (see Appendix S2 for details) using the software package JAGS (Plummer, 2003), which uses Markov chain Monte Carlo (MCMC) to sample from the joint posterior of the model parameters. Depending on the model (main or alternative model), we ran three parallel chains for 100 000–200 000 iterations each. After discarding the first 50% of iterations as 'burn-in', we thinned the chains by 100 to reduce within-chain autocorrelation and to reduce storage requirements; convergence was assessed using the Brooks–Gelman–Rubin diagnostic tool (Gelman *et al*., 2013). This produced roughly 3000 independent samples from the posterior distribution for each parameter, which were summarized by their posterior means, central 95% credible intervals (CIs) defined by the 2.5th and 97.5th percentiles, and Bayesian P-values (Gelman *et al*., 2013).

We assessed the performance of the model by comparing predicted GPP versus observed GPP. We used the coefficient of determination (R^2) as an informal measure of model accuracy. A limitation with solely using R^2 is that it does not detect when overfitting occurs, the phenomenon by which R^2 can increase with greater model complexity (more parameters). To overcome this, we also calculated two other commonly used model assessment diagnostics: the deviance information criterion (DIC) and the posterior predictive loss (PPL). Each of these statistics is the sum of a goodness-of-fit term and a model complexity (penalty) term that describes the effective number of parameters (Gelfand & Ghosh, 1998; Spiegelhalter *et al*., 2002). One model is more desirable over another if it has a lower DIC and lower PPL. Using these two indices, we compared our main model with the alternative model.

Estimates of seasonal, annual, and 6-year GPP

Our Bayesian approach to analyzing the GPP data also provides a framework for predicting GPP for time periods for which it was not measured. Each of the fitted models (main and alternative) was subsequently applied on an hourly time step during the March–October period (we assumed GPP = 0 during other months due to the lack of vegetation during these winter months) for 2007–2012, and for every plot using each of the 3000 parameter sets sampled from the posterior distribution. The model simulations were implemented using Eqns (2–5) as well as all measurements of plot-level data (daily SWC, daily greenness, hourly Tair, hourly VPD, and annual N). The resulting hourly GPP predictions were summed within each season, each year, and across all years for each of the 3000 model executions, yielding posterior predictive distributions of seasonal (spring [March–May], summer [June–August], fall [September–October]), annual (March–October), and 6-year GPP estimates. These distributions account for both model uncertainty (e.g., lack of fit) and parameter uncertainty.

Comparisons to GPP simulated from 12 terrestrial biosphere models

The data-driven predicted GPP values could serve as important 'data products' for informing and evaluating terrestrial biosphere models (TBMs). Importantly, the Bayesian procedure explicitly quantifies uncertainty in such data products. To exemplify the importance of quantification of data product uncertainty, we considered two different types of data products: (i) 6-year cumulative GPP from the main and alternative models as described in the previous subsection, and (ii) the percent change in the 6-year GPP under warming (cT) and eCO_2 (Ct) relative to the control (ct). As with the first, the

second data product was computed using Monte Carlo simulations based on the 3000 posterior estimates of the 6-year GPP (see Appendix S3 for description of how both data products were computed). The 6-year GPP and GPP responses predicted from 12 TBMs were compared against the corresponding data products. The TBMs included: six land surface models (CABLE, CLM4.0, CLM4.5, ISAM, OCN, and ORCHIDEE); three global dynamic vegetation models (JULES, LPJ-GUESS, and SDGVM); and three ecosystem models (DAYCENT, GDAY, and TECO); see Table S1 in the supplementary material for a description of the TBMs. The TBMs were not calibrated to the site using response data, but they were provided optional data or parameter values (e.g., Vcmax, specific leaf area, rooting depth, soil texture) representative of the site. Models were also forced with site meteorological data covering the 6 years of the experiment (see Appendix S4 for details).

As a result of the TBMs not being rigorously calibrated against the PHACE data, there was no expectation that the TBM responses would match or be close to the expected PHACE responses. The purpose of comparing our 'GPP data product' against the TBM output was to illustrate how our data product could be used to inform the TBMs. Our analysis represents a more flexible and potentially more rigorous method for 'gap-filling' missing data – compared to algorithms that are currently used to gap-fill, for example, eddy flux data – and we show how it can be used to generate GPP estimates (data products) over the course of the experiment.

Results

Assessment of model performance

Our main model was able to explain a large portion of the variation in the hourly GPP observations (overall R^2 of 0.79). However, the accuracy of the GPP predictions varied among the treatments (Fig. 1), with treatment-specific fits: cT ($R^2 = 0.86$), ctd ($R^2 = 0.81$), ct ($R^2 = 0.80$), cts ($R^2 = 0.77$), CT ($R^2 = 0.77$), and Ct ($R^2 = 0.67$). For all treatments, the model tends to slightly underpredict GPP at high values, and while

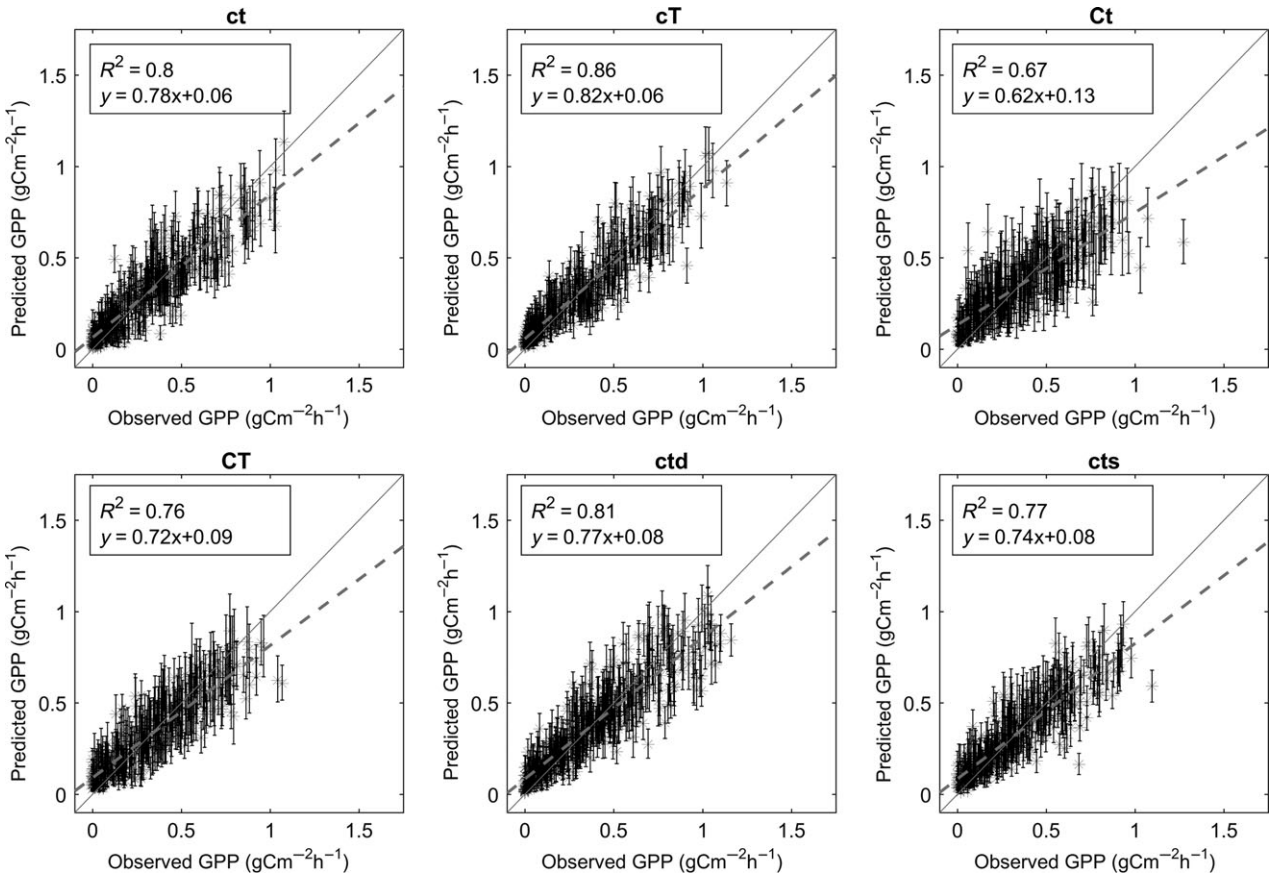

Fig. 1 Observed versus predicted GPP for each treatment. The predicted values were obtained from the main model (with antecedent effects) and are represented by the posterior means and central 95% credible intervals of replicated observations (Gelman *et al*., 2013) of GPP, based on Eqns (1) and (2). The solid, diagonal gray line represents the 1:1 line; the dashed line represents the best fit line. Treatment codes involve combinations of: c (ambient CO_2), C (elevated CO_2), t (no warming), T (warming), d (deep irrigation), or s (shallow irrigation).

this bias is minimal, it is more pronounced in the Ct treatment (Fig. 1). That is, among a number of treatments, there are a handful of measurements that are significantly higher than the modeled values, and these seem to mainly be concentrated on 1 or 2 days during the fall (Fig. S5).

The alternative model, which excluded all of the antecedent covariates, resulted in a poorer fit (R^2 = 0.58 overall, R^2 ranged from 0.40 to 0.67 among treatments) and greater bias (more severe underprediction of GPP at high values) (Fig. S1). The more robust DIC and PPL measures also strongly indicated much better model performance for the main model compared to the alternative model (DIC = 12 690 and PPL = 45 852 for the main model, with DIC = 13 903 and PPL = 80 067 for the alternative model).

Phenology of grassland carbon uptake and its relation to precipitation

The time series of predicted GPP revealed high interannual variability (Fig. 2). For example, for the control treatment (ct), predicted daily GPP reached a maximum around 10 g C m^{-2} day^{-1} for 2009 and 2010, which was double the predicted maximum in 2012 (~5 g C m^{-2} day^{-1}; Fig. 2a). Within years, bimodal peaks in GPP were predicted in 2007, 2008, 2011, and 2012 in response to spring and late-summer precipitation inputs.

Treatment effects on GPP

Over the entire experimental period (2007–2012), the largest and most statistically significant increases in GPP relative to the control treatment (ct) occurred under warming (29% increase; Table 1 and Fig. 3b; P = 0.02 for ct vs. cT), eCO_2 (26%; Table 1 and Fig. 3b; P = 0.07 for ct vs. Ct), and deep irrigation (28%; Table 1 and Fig. 3b; P < 0.01 for ct vs. ctd).

At the annual timescale, relative to ct, annual GPP increased under eCO_2 (Ct) in 2007, 2008, 2011, and 2012 (Fig. 3a and Table 1; ct vs. Ct, P = 0.007, 0.09, 0.02 and 0.009, respectively). Warming (cT) also stimulated annual GPP in 2007, 2008, 2010, and 2011 (Fig. 3a and Table 1; ct vs. cT, P = 0.006, 0.04, 0.09, and 0.005 respectively). There is some evidence that the combination of eCO_2 and warming (CT) enhanced GPP in 2007 and 2011 (Fig. 3a and Table 1; ct vs. CT, P = 0.09 and 0.08, respectively). The large increase in GPP under deep irrigation (ctd) was reflected across individual years, with four showing statistically significant increases of 28–61%. In the absence of warming, annual GPP under eCO_2 (Ct) was similar to annual GPP under shallow irrigation (cts) for all years (Table 1; Ct vs. cts, P > 0.18 for any individual year).

Seasonal differences in the treatment effects emerged. The 29% overall increase in GPP under warming (cT) relative to the control (ct) during all 6 years was

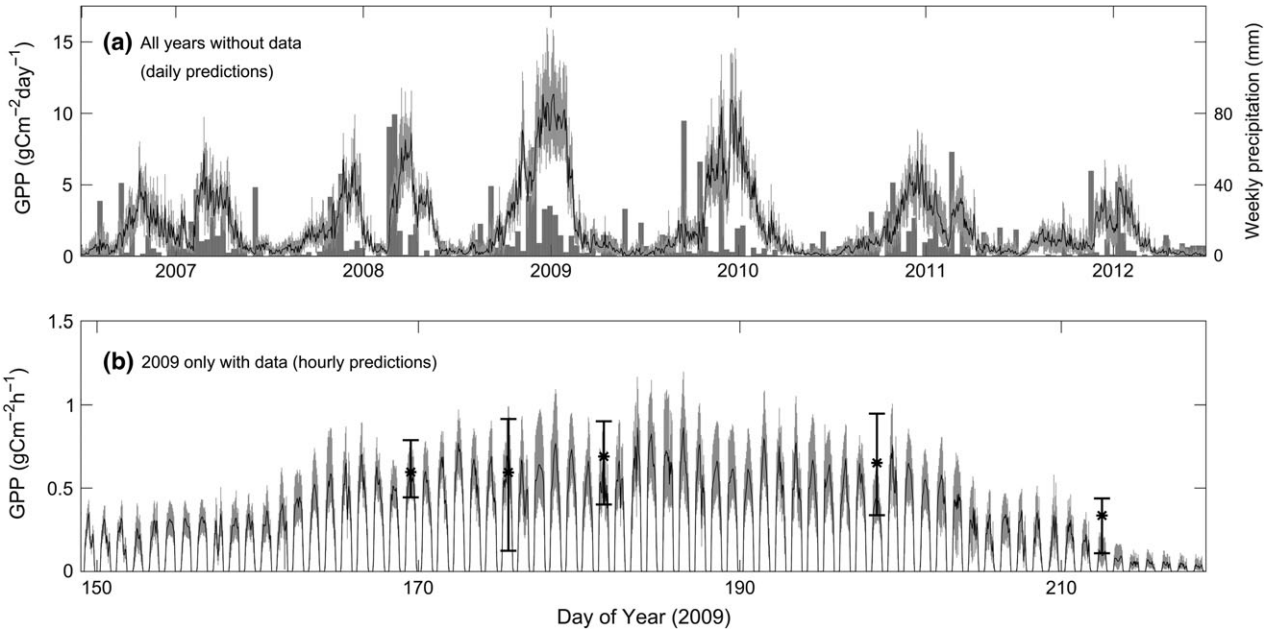

Fig. 2 Time series of predicted gross primary production (GPP) for (a) daily GPP for the control (ct) treatment, where the grey bars denote the weekly precipitation at the site, and (b) hourly GPP for days of the year 140–215 for 2009 for the ct treatment (observed GPP is denoted by *). In both (a) and (b), the black line represents the posterior mean of the daily (a) or hourly (b) predicted GPP, and the grey error bars indicate the 95% credible intervals. The data points and associated error bars in panel (b) represent the mean and range of GPP observations made on measurement days and across at least four of the five plots of the control treatment.

primarily driven by enhanced spring productivity (Fig. 3b, black-filled portion of cT bars; Table 1, ct vs. cT: 129% increase, $P = 0.001$). During the summer, there was on average an 11% decline in GPP under cT (Table 1, ct vs. cT, $P = 0.15$), which is consistent with Pendall *et al.* (2013) who used linear regression and linear interpolation to estimate April–September GPP sums from data. Although the CO_2 effect was only statistically significant ($P < 0.09$) for four of the 6 years, GPP increased by 124% under eCO_2 (Ct) during fall. The spring cT and fall Ct GPP estimates were the only treatment-by-season combinations that were always significantly different ($P < 0.03$) from the corresponding season-level ct estimates, for all years (Table 2, rows 1 and 3). Compared with spring and summer, GPP also increased the most during fall under eCO_2 and warming (ct vs. CT: 42% increase, $P = 0.03$), deep irrigation (ct vs. ctd: 68% increase, $P = 0.002$), and shallow irrigation (ct vs. cts: 66% increase, $P = 0.008$) (Table 1).

Importance of current and antecedent conditions for understanding treatment effects on GPP

Including antecedent terms in the submodels for A_{max} and Q (see Eqn (3)) resulted in decreases in the predicted 6-year GPP relative to the alternative model, with the greatest reductions occurring for the control treatment (by 12%, $P = 0.14$), the eCO_2 × warming treatment (by 20%, $P = 0.04$), and the deep irrigation treatment (by 14%, $P = 0.05$). Furthermore, 34 of the 36 treatment × year combinations corresponded to a decrease in annual GPP of between 1% and 42% for the main model versus the alternative model (Tables S3a, S3b, S3c). Both A_{max} and Q were not significantly affected by concurrent covariates (SWC, VPD, Tair, greenness, and N), for most or all treatments, depending on the covariate (Table 3). Conversely, the main effect of two of the three antecedent covariates (VPD_{ant} and $Tair_{ant}$) on A_{max} was significant for the majority of treatments (Fig. 4a, b; Table 3). The most important

Table 1 Percent differences in predicted annual GPP for key pairs of treatments. Percentages are given for each year, for the 6-year total (2007–2012), and for the 6-year seasonal totals (spring, summer, fall)

	2007	2008	2009	2010	2011	2012	2007–2012	2007–2012 (Spring)	2007–2012 (Summer)	2007–2012 (Fall)
Warming effect (cT – ct)	40**	30*	12	27(†)	50**	29	29*	129**	−11	56**
Elevated CO_2 effect (Ct – ct)	47**	31(†)	−5	7	49	63**	26(†)	47(†)	1	124**
Warming and CO_2 effect (CT – ct)	28(†)	8	−11	−3	24(†)	−1	6	20	−5	42*
Deep irrigation effect (ctd – ct)	30*	30**	15	1	57**	61**	28**	31	19*	68**
Shallow irrigation effect (cts – ct)	29(†)	9	−10	−9	25(†)	41	9	2	2	66**

Asterisks denote the Bayesian *P*-value for the difference: $P \leq 0.01$ (**), $0.01 < P \leq 0.05$ (*), and $0.05 < P \leq 0.1$ ((†)). See Fig. 1 legend for treatment codes.

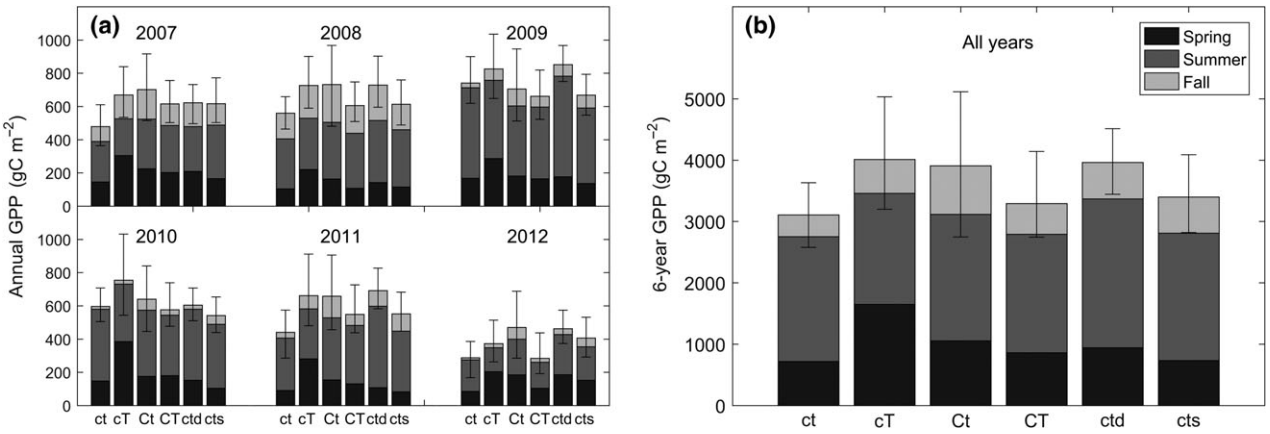

Fig. 3 Predicted annual (growing season; March–October) and seasonal GPP for each treatment by (a) each study year and (b) summed across all 6 years. The overall height of each bar denotes the posterior mean and the error bars represent the central 95% credible intervals of the (a) annual GPP or (b) 6-year GPP. The totals represented by each bar are broken down by seasonal totals according to the shading. See Fig. 1 legend for treatment codes.

Table 2 Percent differences in predicted seasonal GPP for key pairs of treatments, for selected seasons. Pairs of treatments and seasons were selected based on the percent change values in the furthest three right columns of Table 1 that were significant (had asterisks)

	2007	2008	2009	2010	2011	2012	2007-2012
Warming effect (cT – ct) for spring	109**	112**	70**	161**	209**	141**	129**
Warming effect (cT – ct) for fall	60**	27	146*	38	127**	97	56**
eCO_2 effect (Ct – ct) for fall	100**	46*	263**	281*	268**	461**	124**
eCO_2×warming effect (CT – ct) for fall	45(†)	7	129	89	90*	93	42*
Deep irrigation effect (ctd – ct) for summer	11	24*	11	-1	55**	27	19*
Deep irrigation effect (ctd – ct) for fall	60(†)	37*	149(†)	38	168**	177(†)	68**
Surface irrigation effect (cts – ct) for fall	44	-2	175**	208*	196**	315**	66**

As in Table 1, asterisks denote the Bayesian *p*-value for the difference: $p \leq .01$ (**), $0.01 < p \leq .05$ (*) and $.05 < p \leq .1$ ((†)). See Fig. 1 legend for treatment codes.

Table 3 Summary of posterior estimates and Bayesian *P*-values for parameters in the A_{max} and Q functions (α's and β's, respectively; see Eqn 3)

Effect parameter (associated covariate)	Treatment ct	cT	Ct	CT	ctd	cts
α_1 (SWC)	–			+		+
α_2 (VPD)	–					
α_3 (Tair)						
α_4 (SWC_{ant})		+		+		+
α_5 (VPD_{ant})		–	–	–	–	
α_6 ($Tair_{ant}$)		+	+	+	+	
α_7 (Nitrogen)			–			+
α_8 (Greenness)	–				+	
α_9 ($\Delta Greenness_{ant}$)					–	
α_{10} (VPD×Tair)	+					
α_{11} (Tair×Tair)						
α_{12} ($SWC \times SWC_{ant}$)				–		–
α_{13} ($Tair \times Tair_{ant}$)						
α_{14} ($SWC_{ant} \times Tair_{ant}$)	+			+		
α_{15} ($SWC_{ant} \times VPD_{ant}$)	–			–		
β_1 (SWC)	+				+	–
β_2 (VPD)					–	
β_3 (Tair)						
β_4 (SWC_{ant})	+	+			+	
β_5 (VPD_{ant})						
β_6 ($Tair_{ant}$)	+	–				+
β_7 (Greenness)	+					
β_8 ($\Delta Greenness_{ant}$)						
β_9 (VPD×Tair)						
β_{10} (Tair×Tair)		+				
β_{11} ($SWC \times SWC_{ant}$)				+		
β_{12} ($Tair \times Tair_{ant}$)						
β_{13} ($SWC_{ant} \times Tair_{ant}$)		–		–	–	+
β_{14} ($SWC_{ant} \times VPD_{ant}$)	+			+	+	

Dark gray cells indicate $P \leq 0.001$, medium gray indicate $0.001 < P \leq 0.01$, light gray indicate $0.01 < P \leq 0.05$, and white indicate $P > 0.05$. The signs (+ or –) denote a positive or negative effect. See Fig. 1 legend for treatment codes.

predictors for Q involved the $SWC_{ant} \times Tair_{ant}$ and $SWC_{ant} \times VPD_{ant}$ interactions, which were significant for four and three of the treatments, respectively (Fig. 4c, d; Table 3). Although the direction of the VPD_{ant} (for A_{max}), $Tair_{ant}$ (A_{max}), $SWC_{ant} \times Tair_{ant}$ (Q), and $SWC_{ant} \times VPD_{ant}$ (Q) effects was consistent for the vast majority of treatments (Table 3), the magnitude of the antecedent effects differed among certain pairs of treatments (Fig. 4a, c, d).

Given that antecedent conditions are important for understanding GPP, we can evaluate the timescales over which each variable influences GPP. For SWC_{ant}, the first 2 weeks prior to the GPP measurement were generally the most important for predicting GPP (Fig. S2a). For the majority of treatments, Tair experienced 3–4 days prior and VPD from 1 to 3 days prior tended to be the most important for predicting GPP (Fig. S2b, c).

Comparison of predicted 6-year GPP with TBMs

When comparing the GPP predictions from our data-driven analysis with those of 12 terrestrial biosphere models (TBMs), the 95% credible intervals (CIs) of our 6-year GPP 'data product' (whether generated from the main or alternative model) under the control (ct) and eCO_2 (Ct) treatments are fairly narrow compared with the range of TBM predictions (Fig. 5a, b). Under the control treatment, only one of the twelve TBM predictions fell within the 95% CI of the data product if antecedent conditions were included in the calculation of the data product (Fig. 5a, black cross and error bar). The number of TBM predictions consistent, or almost so, with the data product increased to five if antecedent conditions were not included when computing the data product (Fig. 5a, gray cross and error bar). Under the eCO_2 scenario, there was greater similarity in the number of TBM predictions agreeing with the data product if antecedent versus no antecedent conditions were included for determining the data product (Fig. 5b).

The TBMs also need to accurately predict the relative change in GPP under scenarios of environmental change (e.g., eCO_2, warming, or some combination). We used our GPP analysis framework to produce a data product of the percent difference

in GPP under treatment conditions relative to control conditions. In contrast to the cumulative GPP estimates, these percent differences were associated with high uncertainty, sometimes spanning both decreases and increases (e.g., Fig. 5c, d). This resulted in the majority of TBM simulations that are consistent with this data product (i.e., the TBM predictions lie within the CIs; Fig. 5c, d), despite the wide range of TBM predictions. Thus, the data product associated with GPP on the absolute scale (Fig. 3a, b) is more useful for evaluating and informing TBMs than the data product on the percent change scale (e.g. Fig. 3c, d).

Discussion

Implications of treatment effects on annual GPP

Annual GPP was predicted to be most stimulated by elevated CO_2 (eCO_2, Ct treatment) during the three

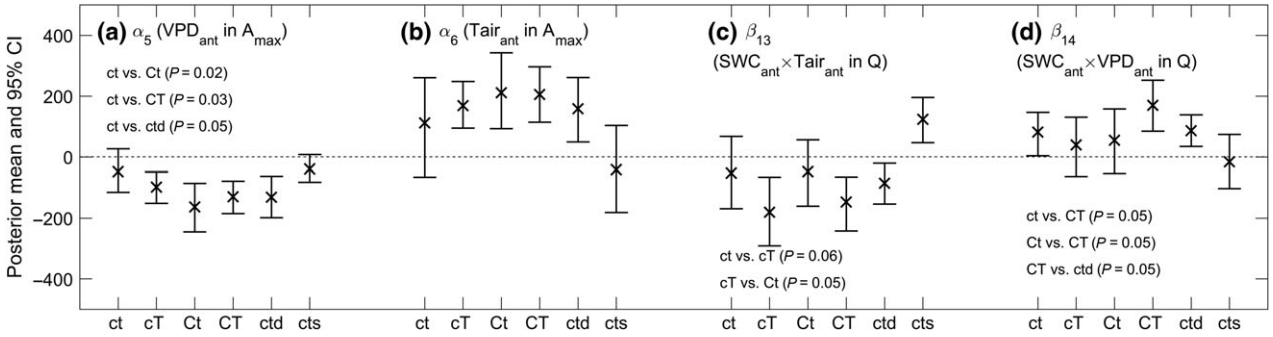

Fig. 4 Posterior means (denoted by ×) and central 95% credible intervals (CIs; error bars) for a subset of parameters (covariate effects) in the A_{max} function (panels a and b) and the Q function (panels c and d) (Eqn 3, Table 2); these parameters were the most significant across the greatest number of treatments. The key A_{max} parameters are associated with antecedent vapor pressure deficit (VPD_{ant}) and antecedent air temperature ($Tair_{ant}$). The key Q parameters are associated with antecedent soil water content (SWC_{ant}) and the interaction between SWC_{ant} and VPD_{ant}. 95% CIs that overlap with zero (dashed horizontal line) indicate a nonsignificant effect. See Fig. 1 legend for treatment codes.

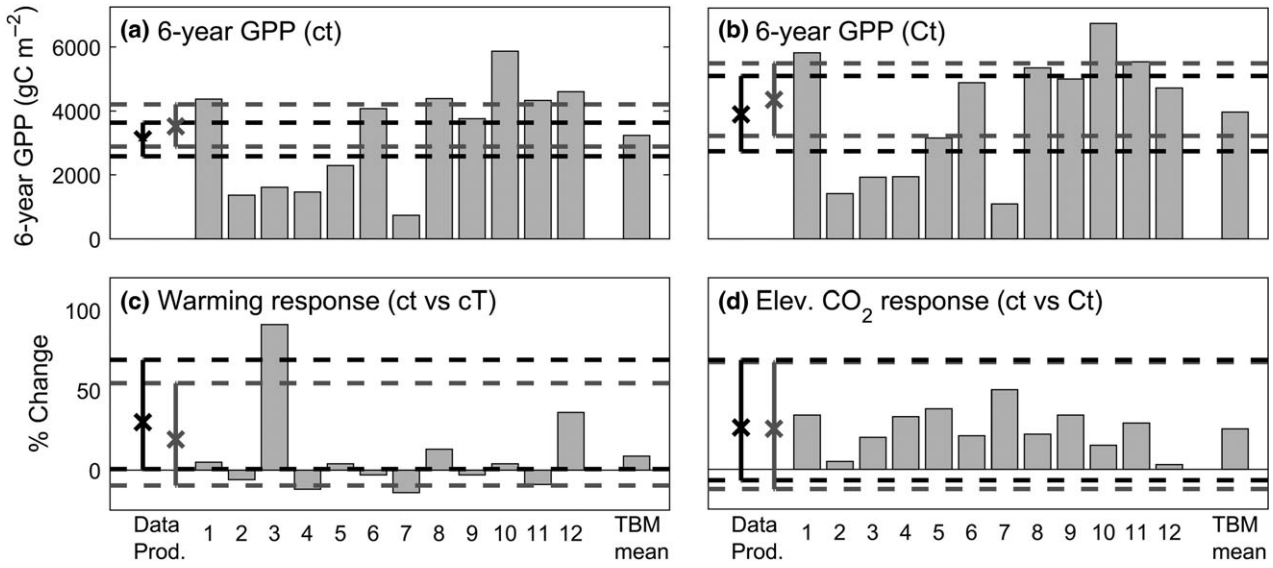

Fig. 5 Comparison of the posterior estimates of GPP ('data product'; × = posterior mean; error bars and horizontal dashed lines = 95% credible interval) with simulated GPP from 12 terrestrial biosphere models (TBMs; see Table S1 in the supplementary information for descriptions of each TBM, labeled 1–12). The GPP data products are based on the GPP posterior estimates generated from the main (black lines and symbols) and alternative (gray lines and symbols) models, where the alternative model is the same as the main model but without antecedent effects. The metrics shown here are as follows: total 6-year GPP (2007–2012; growing season, March–October in each year) under (a) the control (ct) treatment and (b) the elevated CO_2 (Ct) treatment; and percentage change in total 6-year GPP under (c) warming (cT) relative to ct, and (d) Ct relative to ct.

driest years of our study (2007, 2011, and 2012), suggesting that increased GPP under eCO_2 could have resulted from enhanced water-use efficiency (Kelly *et al.*, 2015). The shallow irrigation (cts) treatment confirmed the role of SWC in mediating the GPP responses to eCO_2, consistent with findings in a similar grassland system (Parton *et al.*, 2012). Moreover, deep irrigation led to a greater percentage increase in GPP compared with eCO_2 or surface irrigation (Table 1; Fig. 3). This may reflect the frequency and magnitude in which irrigation was applied under ctd (twice, large events) compared with cts (three-five smaller events). Larger, less frequent precipitation events are expected to stimulate GPP to a greater extent than smaller, more frequent events, especially early in the growing season (Lauenroth & Sala, 1992; Heisler-White *et al.*, 2008; Ogle *et al.*, 2015). A prior estimate of annual GPP for this same site suggested a reduction in GPP by eCO_2 in 2009 (Pendall *et al.*, 2013), but our analysis revealed that a significant difference existed only during summer of that year ($P = 0.06$). We also found that 2009 – the wettest year – had the highest annual GPP under the control treatment compared with all other study years (Fig. 3, Tables S2 and S3a), in agreement with Mueller *et al.* (2016) who found the highest aboveground biomass in that year but no eCO_2 effect. Other grassland studies have found no response or a reduction in primary production under eCO_2 during wet years (Polley *et al.*, 2013; Hovenden *et al.*, 2014).

Climate change treatments altered the seasonality of GPP, particularly in spring and fall, as observed for species- and community-level measurements at the same site (Reyes-Fox *et al.*, 2014; Zelikova *et al.*, 2015). Across all years, warming (cT) consistently increased annual GPP by 12–50%, and this was predominantly driven by enhanced production during the spring (Fig. 3a; Tables 1 and 2), when temperature limits constrained productivity in this high-elevation system. Increased annual GPP for all treatments, except cT, relative to the control (ct) was dominated by increases in GPP during the fall (Table 1, furthest right column). The consistency of the statistical significance of this eCO_2 enhancement during fall of most years, as well as the warming enhancement in spring (Table 2), may be due to two potential co-occurring mechanisms: (i) Spring warming directly stimulates earlier snow melt, photosynthesis, and plant growth (Figs. S4, Luo, 2007; Sherry *et al.*, 2008; Richardson *et al.*, 2010); and/or (ii) the SWC in fall is sustained for longer as a result of the water-saving effects of eCO_2 in water-limited systems like at PHACE (Morgan *et al.*, 2004, 2011; Nowak *et al.*, 2004; Webb *et al.*, 2012). Our results indicate that these GPP enhancements in spring and fall may extend the growing season. For example, in 2008 (an average year in terms of meteorology), modeled GPP during spring was consistently higher under warming, although observed GPP showed only a minor increase (Fig. S5a, c). In fall, modeled GPP remained significantly higher with eCO_2 compared with ambient, which is supported by the observations (Fig S5b, d). In the warm, dry year of 2012, GPP was significantly enhanced by warming in spring and by eCO_2 in fall (Table 3). This is partly consistent with observed treatment effects on vegetation greenness (Zelikova *et al.*, 2015), which was stimulated by the combination of warming and eCO_2 in spring of 2012. Overall, our data model product provides reasonable support for hypothesized mechanisms that could extend the growing season in this cool, dry grassland, although additional observations in spring and fall could improve confidence in climate change effects on ecosystem physiology (Richardson *et al.*, 2010, 2013).

Importance of antecedent conditions for predicting GPP and evaluating treatment differences

An increasing number of studies recognize the importance of antecedent conditions in understanding the terrestrial C cycle (Gamnitzer *et al.*, 2011; Cable *et al.*, 2013; Barron-Gafford *et al.*, 2014; Ryan *et al.*, 2015). Our main model (with antecedent effects) explained 67–86% of the variation in the GPP data, but the alternative model (without antecedent effects) only explained 40–67% of the variation. This difference in the explanatory power of models that include antecedent conditions has also been demonstrated for other C flux components, including soil respiration (Barron-Gafford *et al.*, 2014; Ogle *et al.*, 2015), annual aboveground NPP, and annual tree growth (Ogle *et al.*, 2015). The increased explanatory power of the 'antecedent models' cannot not be solely explained by the additional parameters that they introduce given the support conveyed by model selection indices that penalize for the number of parameters or model complexity. In particular, our results suggest that antecedent vapor pressure deficit (VPD_{ant}) and antecedent air temperature ($Tair_{ant}$) were the most important predictors of GPP, primarily via their effects on maximum potential GPP (A_{max}). Antecedent SWC (SWC_{ant}) interacted with these two factors to affect light-use efficiency (Q).

The importance of $Tair_{ant}$ suggests that accounting for seasonal changes in air temperature is critical for obtaining good estimations of A_{max} in this temperate grassland, especially in spring when moisture is less limiting (Lauenroth & Sala, 1992). The importance of antecedent temperature has been implicated as depicting a temperature acclimation response (Ogle *et al.*, 2015). However, the general positive effect of $Tair_{ant}$ on

A_{max} actually indicates that warmer past temperatures tend to enhance A_{max} and GPP, regardless of the current air temperature which appears to have little impact on GPP once antecedent temperature is accounted for (see Table 3). It appears that GPP is more likely to respond to concurrent changes in soil water (SWC), and to some extent VPD, compared with temperature. The importance of concurrent SWC and VPD on GPP likely reflects stomatal regulation of plant water status, which in turn is expected to affect photosynthesis, and thus GPP.

While we would expect GPP to be partly regulated by short-term (sub-daily) changes in VPD (e.g., via stomatal control; Oren *et al.* 1999), we also found that VPD experienced over the past few days (VPD_{ant}) affects GPP, especially through its influence on A_{max}. In particular, high VPD for about 1–3 days prior is predicted to reduce A_{max}, across all treatments (Fig. 4a). While the effect of VPD on stomatal closure and photosynthesis is usually treated as being instantaneous due to tight coupling of stomatal conductance to VPD (Collatz *et al.*, 1991), this study suggests that plants may adjust to VPD over longer timescales. VPD conditions occurring over the past 1–7 days represent a proxy for past atmospheric drought conditions (Haddad *et al.*, 2002), and GPP is likely to be negatively impacted by cumulative atmospheric drought. Furthermore, the VPD_{ant} effect was more negative under eCO_2 (Fig. 4a), indicating greater sensitivity of stomata (and hence, photosynthesis) to atmospheric drought, potentially leading to higher integrated water-use efficiency under eCO_2.

The use of VPD as a predictor of GPP is not new (Groenendijk *et al.*, 2011), but the proposition that antecedent VPD is an important driver of GPP has not been previously considered. One possibility is that this effect is just an artifact of our model because VPD depends upon Tair, and the VPD_{ant} effect could reflect a nonlinear $Tair_{ant}$ effect. However, this is unlikely because although current VPD is highly correlated with current Tair ($r = 0.85$), the correlation between the antecedent covariates (VPD_{ant} versus $Tair_{ant}$) is weaker ($r = 0.68$). Furthermore, our model contains quadratic Tair ($Tair^2$) terms in both the A_{max} and Q functions, and thus, the shape of the expected response of GPP to Tair (peaked) should already be accounted for. A more plausible explanation for the VPD_{ant} effect is that stomatal conductance or photosynthesis acclimates to VPD. For example, Kutsch *et al.* (2001) found that a decrease in stomatal aperture in beech trees – implying a decrease in GPP – was negatively correlated with the previous month's mean VPD. The importance of past VPD, rather than past SWC, prompted the authors to suggest that plants possess a biochemical memory of past climatic conditions. Buckley (2005) further suggests that when VPD exceeds some threshold, water potential can reach a cavitation threshold, leading to cavitation and reducing transpiration at any given VPD. If VPD is subsequently reduced, then there is a lag between the recovery of water potential and embolism repair; the timescale of this recovery is not well understood but could contribute to a GPP versus VPD lag. Various mechanisms have been proposed to explain the stomatal behavior versus VPD lag including the hydroactive feedback hypothesis (Buckley 2016) or delays associated with abscisic acid (ABA) signaling (Aliniaeifard & van Meeteren, 2014). Clearly, additional research is required to establish the generality of a GPP versus VPD lag (antecedent effect) and to identify underlying mechanisms related to stomatal behavior, biochemical acclimation, or other explanations.

Terrestrial biosphere models (TBMs) do not commonly account for the potential direct effects of antecedent VPD on the physiological components, for example, through acclimation of photosynthesis (Kattge & Knorr, 2007; Smith *et al.*, 2015). Nevertheless, soil water content does contain information on antecedent VPD, and thus via soil water effects on physiology models have an indirect 'memory' of VPD. However, model physiological responses to changes in soil water are empirical and can range from insensitive to too sensitive (De Kauwe *et al.*, 2014, 2015). First principles methods that integrate carbon costs and benefits under antecedent environmental conditions (Mueller *et al.*, 2016; De Kauwe *et al.*, in press) may provide a robust method to incorporate acclimation of leaf physiology to antecedent VPD and soil water into TBMs. Our results highlight accounting for such an acclimation process, which directly considers the effect of antecedent conditions, could improve modeled estimates of photosynthesis.

Implications for the terrestrial carbon cycle

Estimates of global GPP used in the last IPCC report were calculated from site-level GPP estimates that were derived by fitting a light response curve to flux tower NEE data (Beer *et al.*, 2010; Lasslop *et al.*, 2010). The site-level A_{max} terms in these analyses were also represented as exponential functions of current environmental covariates (Lasslop *et al.*, 2010). If antecedent conditions (such as VPD_{ant}, SWC_{ant}, and $Tair_{ant}$) had been included, our analysis suggests that annual estimates of GPP at semiarid grasslands could have been improved (Fig. 1 vs. Fig. S1). For other ecosystems or plant functional types that are less sensitive to drought, the effect of antecedent meteorological conditions may be less pronounced. Moreover, our results show that including antecedent conditions could result in lower

estimates of cumulative GPP in temperate grasslands under current climate (by 12%), and especially under a future, warmer climate and eCO_2 (by 20%; see Table S3c).

Since the early 1990s, global change experiments, such as Free Air CO_2 Enrichment (FACE) studies, have generated data on responses of key biogeochemical processes to future environmental conditions. Such experiments have become invaluable for informing model forecasts (Piao *et al*., 2013; Zaehle *et al*., 2014; De Kauwe *et al*., 2014; Walker *et al*., 2014; De Kauwe *et al*., in press). One of the challenges associated with applying terrestrial biosphere models (TBMs) to understand climate change impacts on GPP and the C cycle is limited access to accurate data products for informing and evaluating the models. As many data products are derived from simpler models that are fit to observational data, it is prudent to account for uncertainty in such data products because they are not perfect representations of the real system. Our hierarchical Bayesian approach to analyzing the GPP data in the context of a fairly simple light-response model provides a mechanism for predicting GPP at nonmeasurement time periods, while accounting for uncertainty in these predictions. However, we wish to emphasize that the purpose of the comparison between TBMs and our 'data product' (Fig. 5) was not to validate the TBMs, but rather to evaluate the utility of the data products.

We are confident in our seasonal, annual, and 6-year cumulative GPP predictions given their relatively narrow 95% CIs (e.g., Fig. 5a and 3b). The width of the intervals, however, did vary among global change treatments, with the widest intervals (and weakest model fits [lowest R^2s]) occurring for treatments involving eCO_2 (Ct and CT). This suggests that additional information or improved model structure is required to obtain more accurate GPP estimates under eCO_2. In general, the tight estimates for cumulative GPP at different timescales suggest that this would be a valuable (semi-)independent data stream that TBMs can be compared against.

The importance of antecedent environmental conditions on grassland GPP has been highlighted by the Bayesian model selection procedure used in this study. Antecedent conditions were key predictors of GPP, in particular air temperature and vapor pressure deficit of the past week, and research into the mechanism by which antecedent Tair and VPD affect GPP would be an interesting and useful contribution to understanding the carbon cycle in these grassland ecosystems. Including antecedent conditions substantially improved the fit of the Bayesian model and led to a consistent reduction in the computed multiyear GPP in this grassland ecosystem, across the vast majority of treatments and years. Given the global coverage of grassland ecosystems, understanding the effect of antecedent environmental conditions more broadly is likely to have implications for our understanding of the global carbon cycle.

Data availability

Data are available through the digital repository, Dryad. Please e-mail Elise Pendall (E.Pendall@westernsydney.edu.au) or Edmund Ryan (edmund.ryan@lancaster.ac.uk) for details.

Acknowledgements

This material is based upon work supported by the US Department of Agriculture, Agricultural Research Service Climate Change, Soils & Emissions Program, USDA-CSREES Soil Processes Program (#2008-35107-18655), US Department of Energy Office of Science (BER), through the Terrestrial Ecosystem Science program (#DE-SC0006973), and the Western Regional Center of the National Institute for Climatic Change Research, and by the National Science Foundation (DEB#1021559). Any opinions, findings, and conclusions or recommendations expressed in this material are those of the author(s) and do not necessarily reflect the views of the National Science Foundation. We thank D. LeCain, J.A. Morgan, J. Heisler-White, A. Brennan, S. Bachman, Y. Sorokin, T.J. Zelikova, D. Blumenthal, K. Mueller, and numerous others for assistance in data collection and operation of PHACE facilities, and B. Yang for use of his gap-filled meteorological data at the site. We also thank D. Kinsman for his helpful comments on the discussion section.

Author contributions

ER, KO, and EP designed the study; ER conducted the analysis and wrote the manuscript, with contributions from KO, EP, AW, MDK, and BM. The Bayesian analysis was directed by KO; DP assisted with implementing the Bayesian models. The remaining authors provided GPP model output from eight of the TBMs in order to construct Fig. 5.

References

Acock B, Hand D, Thornley J, Wilson JW (1976) Photosynthesis in stands of green peppers. An application of empirical and mechanistic models to controlled-environment data. *Annals of Botany*, **40**, 1293–1307.

Ainsworth EA, Long SP (2005) What have we learned from 15 years of free-air CO_2 enrichment (FACE)? A meta-analytic review of the responses of photosynthesis, canopy properties and plant production to rising CO_2. *New Phytologist*, **165**, 351–372.

Aliniaeifard S, van Meeteren U (2014) Natural variation in stomatal response to closing stimuli among *Arabidopsis thaliana* accessions after exposure to low VPD as a tool to recognize the mechanism of disturbed stomatal functioning. *Journal of Experimental Botany*, **65**, 6529–6542.

Arora VK, Boer GJ, Friedlingstein P *et al*. (2013) Carbon–concentration and carbon–climate feedbacks in CMIP5 earth system models. *Journal of Climate*, **26**, 5289–5314.

Arp W (1991) Effects of source-sink relations on photosynthetic acclimation to elevated CO_2. *Plant, Cell & Environment*, **14**, 869–875.

Bachman S, Heisler-White JL, Pendall E, Williams DG, Morgan JA, Newcomb J (2010) Elevated carbon dioxide alters impacts of precipitation pulses on ecosystem photosynthesis and respiration in a semi-arid grassland. *Oecologia*, **162**, 791–802.

Barron-Gafford GA, Scott RL, Jenerette GD, Huxman TE (2011) The relative controls of temperature, soil moisture, and plant functional group on soil CO_2 efflux at diel, seasonal, and annual scales. *Journal of Geophysical Research: Biogeosciences* (2005–2012), 116, G01023.

Barron-Gafford GA, Cable JM, Bentley LP, Scott RL, Huxman TE, Jenerette GD, Ogle K (2014) Quantifying the timescales over which exogenous and endogenous conditions affect soil respiration. *New Phytologist*, **202**, 442–454.

Beer C, Reichstein M, Tomelleri E *et al.* (2010) Terrestrial gross carbon dioxide uptake: global distribution and covariation with climate. *Science*, **329**, 834–838.

Bernacchi C, Singsaas E, Pimentel C, Portis A Jr, Long S (2001) Improved temperature response functions for models of Rubisco limited photosynthesis. *Plant, Cell & Environment*, **24**, 253–259.

Buckley TN (2005) The control of stomata by water balance. *New Phytologist*, **168**, 275–291.

Buckley TN (2016) Stomatal responses to humidity: has the 'black box' finally been opened? *Plant, cell & environment*, **39**, 482–484.

Cable JM, Ogle K, Barron-Gafford GA *et al.* (2013) Antecedent conditions influence soil respiration differences in shrub and grass patches. *Ecosystems*, **16**, 1230–1247.

Carrillo Y, Dijkstra FA, Lecain D, Morgan JA, Blumenthal D, Waldron S, Pendall E (2014) Disentangling root responses to climate change in a semiarid grassland. *Oecologia*, **175**, 699–711.

Chapin FS III, Woodwell GM, Randerson JT *et al.* (2006) Reconciling carbon-cycle concepts, terminology, and methods. *Ecosystems*, **9**, 1041–1050.

Ciais P, Sabine C, Bala G *et al.* (2014) Carbon and other biogeochemical cycles. *Climate Change 2013: The Physical Science Basis. Contribution of Working Group I to the Fifth Assessment Report of the Intergovernmental Panel on Climate Change*. Cambridge University Press, Cambridge, pp. 465–570.

Collatz GJ, Ball JT, Grivet C, Berry JA (1991) Physiological and environmental regulation of stomatal conductance, photosynthesis and transpiration: a model that includes a laminar boundary layer. *Agricultural and Forest Meteorology*, **54**, 107–136.

Collins M, Knutti R, Arblaster J *et al.* (2013) Long-term climate change: projections, commitments and irreversibility. *Climate Change 2013: The Physical Science Basis. IPCC Working Group I Contribution to the Fifth Assessment Report of the Intergovernmental Panel of Climate Change*. Cambridge University Press, Cambridge, pp.1029–1136.

Cox PM, Betts RA, Jones CD, Spall SA, Totterdell IJ (2000) Acceleration of global warming due to carbon-cycle feedbacks in a coupled climate model. *Nature*, **408**, 184–187.

De Kauwe M, Medlyn BE, Walker AP *et al.* (in press) Challenging terrestrial biosphere models with data from the long-term multi-factor prairie heating and CO_2 enrichment experiment. *Global Change Biology*.

Desai AR, Richardson AD, Moffat AM *et al.* (2008) Cross-site evaluation of eddy covariance GPP and RE decomposition techniques. *Agricultural and Forest Meteorology*, **148**, 821–838.

Dieleman WI, Vicca S, Dijkstra FA *et al.* (2012) Simple additive effects are rare: a quantitative review of plant biomass and soil process responses to combined manipulations of CO_2 and temperature. *Global Change Biology*, **18**, 2681–2693.

Dukes JS, Chiariello NR, Cleland EE *et al.* (2005) Responses of grassland production to single and multiple global environmental changes. *PLoS Biology*, **3**, e319.

Falge E, Baldocchi D, Olson R *et al.* (2001) Gap filling strategies for defensible annual sums of net ecosystem exchange. *Agricultural and Forest Meteorology*, **107**, 43–69.

Farquhar G, von Caemmerer SV, Berry J (1980) A biochemical model of photosynthetic CO_2 assimilation in leaves of C3 species. *Planta*, **149**, 78–90.

Fay PA, Carlisle JD, Knapp AK, Blair JM, Collins SL (2003) Productivity responses to altered rainfall patterns in a C4-dominated grassland. *Oecologia*, **137**, 245–251.

Friedlingstein P, Cox P, Betts R *et al.* (2006) Climate-carbon cycle feedback analysis: results from the C4MIP model intercomparison. *Journal of Climate*, **19**, 3337–3353.

Friedlingstein P, Meinshausen M, Arora VK, Jones CD, Anav A, Liddicoat SK, Knutti R (2014) Uncertainties in CMIP5 climate projections due to carbon cycle feedbacks. *Journal of Climate*, **27**, 511–526.

Gamnitzer U, Moyes A, Bowling D, Schnyder H (2011) Measuring and modelling the isotopic composition of soil respiration: insights from a grassland tracer experiment. *Biogeosciences*, **8**, 1333–1350.

Gelfand AE, Ghosh SK (1998) Model choice: a minimum posterior predictive loss approach. *Biometrika*, **85**, 1–11.

Gelman A, Carlin JB, Stern HS, Dunson DB, Vehtari A, Rubin DB (2013) *Bayesian Data Analysis*. CRC Press, Boca Raton, FL.

Groenendijk M, Dolman A, Ammann C *et al.* (2011) Seasonal variation of photosynthetic model parameters and leaf area index from global Fluxnet eddy covariance data. *Journal of Geophysical Research: Biogeosciences* (2005–2012), **116**, G04027.

Haddad NM, Tilman D, Knops JM (2002) Long-term oscillations in grassland productivity induced by drought. *Ecology Letters*, **5**, 110–120.

Heisler-White JL, Knapp AK, Kelly EF (2008) Increasing precipitation event size increases aboveground net primary productivity in a semi-arid grassland. *Oecologia*, **158**, 129–140.

Hovenden MJ, Newton PC, Wills KE (2014) Seasonal not annual rainfall determines grassland biomass response to carbon dioxide. *Nature*, **511**, 583–586.

Huxman TE, Snyder KA, Tissue D *et al.* (2004) Precipitation pulses and carbon fluxes in semiarid and arid ecosystems. *Oecologia*, **141**, 254–268.

Jasoni RL, Smith SD, Arnone JA (2005) Net ecosystem CO_2 exchange in Mojave Desert shrublands during the eighth year of exposure to elevated CO_2. *Global Change Biology*, **11**, 749–756.

Kattge J, Knorr W (2007) Temperature acclimation in a biochemical model of photosynthesis: a reanalysis of data from 36 species. *Plant, Cell & Environment*, **30**, 1176–1190.

De Kauwe MG, Medlyn BE, Zaehle S *et al.* (2014) Where does the carbon go? A model–data intercomparison of vegetation carbon allocation and turnover processes at two temperate forest free-air CO_2 enrichment sites. *New Phytologist*, **203**, 883–899.

De Kauwe M, Zhou S-X, Medlyn B, Pitman A, Wang Y-P, Duursma R, Prentice I (2015) Do land surface models need to include differential plant species responses to drought? Examining model predictions across a latitudinal gradient in Europe. *Biogeosciences Discussions*, **12**, 7503–7518.

Kelly JW, Duursma RA, Atwell BJ, Tissue DT, Medlyn BE (2015) Drought× CO_2 interactions in trees: a test of the low-intercellular CO_2 concentration (Ci) mechanism. *New Phytologist*, **209**, 1600–1612.

Kimball B (2005) Theory and performance of an infrared heater for ecosystem warming. *Global Change Biology*, **11**, 2041–2056.

Knapp AK, Smith MD (2001) Variation among biomes in temporal dynamics of aboveground primary production. *Science*, **291**, 481–484.

Kutsch WL, Herbst M, Vanselow R, Hummelshoj P, Jensen NO, Kappen L (2001) Stomatal acclimation influences water and carbon fluxes of a beech canopy in northern Germany. *Basic and Applied Ecology*, **2**, 265–281.

Landsberg J, Waring R (1997) A generalised model of forest productivity using simplified concepts of radiation-use efficiency, carbon balance and partitioning. *Forest Ecology and Management*, **95**, 209–228.

Lasslop G, Reichstein M, Papale D *et al.* (2010) Separation of net ecosystem exchange into assimilation and respiration using a light response curve approach: critical issues and global evaluation. *Global Change Biology*, **16**, 187–208.

Lauenroth W, Sala OE (1992) Long-term forage production of North American shortgrass steppe. *Ecological Applications*, **2**, 397–403.

Luo Y (2007) Terrestrial carbon-cycle feedback to climate warming. *Annual Review of Ecology Evolution and Systematics*, **38**, 683–712.

Luo Y, Medlyn B, Hui D, Ellsworth D, Reynolds J, Katul G (2001) Gross primary productivity in duke forest: modeling synthesis of CO_2 experiment and eddy–flux data. *Ecological Applications*, **11**, 239–252.

Luo Y, Hui D, Zhang D (2006) Elevated CO_2 stimulates net accumulations of carbon and nitrogen in land ecosystems: a meta-analysis. *Ecology*, **87**, 53–63.

Luo Y, Gerten D, le Maire G *et al.* (2008) Modeled interactive effects of precipitation, temperature, and [CO_2] on ecosystem carbon and water dynamics in different climatic zones. *Global Change Biology*, **14**, 1986–1999.

Magnani F, Mencuccini M, Borghetti M *et al.* (2007) The human footprint in the carbon cycle of temperate and boreal forests. *Nature*, **447**, 849–851.

McLeod A, Long S (1999) Free-air carbon dioxide enrichment (FACE) in global change research: a review. *Advances in Ecological Research*, **28**, 1–56.

Medlyn BE, Duursma RA, Eamus D *et al.* (2011) Reconciling the optimal and empirical approaches to modelling stomatal conductance. *Global Change Biology*, **17**, 2134–2144.

Miglietta F, Hoosbeek M, Foot J *et al.* (2001) Spatial and temporal performance of the MiniFACE (Free Air CO_2 enrichment) system on bog ecosystems in northern and central Europe. *Environmental Monitoring and Assessment*, **66**, 107–127.

Morgan JA, Lecain DR, Mosier AR, Milchunas DG (2001) Elevated CO_2 enhances water relations and productivity and affects gas exchange in C3 and C4 grasses of the Colorado shortgrass steppe. *Global Change Biology*, **7**, 451–466.

Morgan J, Pataki DE, Körner C *et al.* (2004) Water relations in grassland and desert ecosystems exposed to elevated atmospheric CO_2. *Oecologia*, **140**, 11–25.

Morgan JA, Lecain DR, Pendall E *et al.* (2011) C4 grasses prosper as carbon dioxide eliminates desiccation in warmed semi-arid grassland. *Nature*, **476**, 202–205.

Mueller K, Blumenthal DM, Pendall E *et al*. (2016) Impacts of warming and elevated CO_2 on a semi-arid grassland are non-additive, shift with precipitation, and reverse over time. *Ecology Letters*, **19**, 956–966.

Norby RJ, Luo Y (2004) Evaluating ecosystem responses to rising atmospheric CO_2 and global warming in a multi-factor world. *New Phytologist*, **162**, 281–293.

Norby RJ, Zak DR (2011) Ecological lessons from free-air CO_2 enrichment (FACE) experiments. *Annual Review of Ecology, Evolution, and Systematics*, **42**, 181.

Nowak RS, Ellsworth DS, Smith SD (2004) Functional responses of plants to elevated atmospheric CO_2–do photosynthetic and productivity data from FACE experiments support early predictions? *New Phytologist*, **162**, 253–280.

Ogle K, Barber JJ, Barron-Gafford GA *et al*. (2015) Quantifying ecological memory in plant and ecosystem processes. *Ecology Letters*, **18**, 221–235.

Oikawa P, Grantz D, Chatterjee A, Eberwein J, Allsman L, Jenerette G (2014) Unifying soil respiration pulses, inhibition, and temperature hysteresis through dynamics of labile soil carbon and O2. *Journal of Geophysical Research: Biogeosciences*, **119**, 521–536.

Oren R, Phillips N, Ewers BE, Pataki DE, Megonigal JP (1999) Sap-flux-scaled transpiration responses to light, vapor pressure deficit, and leaf area reduction in a flooded Taxodium distichum forest. *Tree Physiology*, **19**, 337–347.

Parton W, Morgan J, Smith D *et al*. (2012) Impact of precipitation dynamics on net ecosystem productivity. *Global Change Biology*, **18**, 915–927.

Pendall E, Heisler-White JL, Williams DG, Dijkstra FA, Carrillo Y, Morgan JA, Lecain DR (2013) Warming reduces carbon losses from grassland exposed to elevated atmospheric carbon dioxide. *PLoS ONE*, **8**, e71921.

Piao S, Ciais P, Friedlingstein P *et al*. (2008) Net carbon dioxide losses of northern ecosystems in response to autumn warming. *Nature*, **451**, 49–52.

Piao S, Sitch S, Ciais P *et al*. (2013) Evaluation of terrestrial carbon cycle models for their response to climate variability and to CO_2 trends. *Global Change Biology*, **19**, 2117–2132.

Plummer M (2003) *JAGS: A program for analysis of Bayesian graphical models using Gibbs sampling*. Proceedings of the 3rd International Workshop on Distributed Statistical Computing. Technische Universit, Wien, 125.

Polley HW, Briske DD, Morgan JA, Wolter K, Bailey DW, Brown JR (2013) Climate change and North American rangelands: trends, projections, and implications. *Rangeland Ecology and Management*, **66**, 493–511.

Reich PB, Oleksyn J, Wright IJ (2009) Leaf phosphorus influences the photosynthesis–nitrogen relation: a cross-biome analysis of 314 species. *Oecologia*, **160**, 207–212.

Reyes-Fox M, Steltzer H, Trlica M, McMaster GS, Andales AA, Lecain DR, Morgan JA (2014) Elevated CO_2 further lengthens growing season under warming conditions. *Nature*, **510**, 259–262.

Richardson AD, Black TA, Ciais P *et al*. (2010) Influence of spring and autumn phenological transitions on forest ecosystem productivity. *Philosophical Transactions of the Royal Society of London B: Biological Sciences*, **365**, 3227–3246.

Richardson AD, Keenan TF, Migliavacca M, Ryu Y, Sonnentag O, Toomey M (2013) Climate change, phenology, and phenological control of vegetation feedbacks to the climate system. *Agricultural and Forest Meteorology*, **169**, 156–173.

Roy J, Mooney HA, Saugier B (2001) *Terrestrial Global Productivity*. Academic Press, San Diego, CA.

Rustad LE (2008) The response of terrestrial ecosystems to global climate change: towards an integrated approach. *Science of the Total Environment*, **404**, 222–235.

Rustad L, Campbell J, Marion G *et al*. (2001) A meta-analysis of the response of soil respiration, net nitrogen mineralization, and aboveground plant growth to experimental ecosystem warming. *Oecologia*, **126**, 543–562.

Ryan EM, Ogle K, Zelikova TJ, Lecain DR, Williams DG, Morgan JA, Pendall E (2015) Antecedent moisture and temperature conditions modulate the response of ecosystem respiration to elevated CO_2 and warming. *Global Change Biology*, **21**, 2588–2602.

Schwinning S, Sala OE, Loik ME, Ehleringer JR (2004) Thresholds, memory, and seasonality: understanding pulse dynamics in arid/semi-arid ecosystems. *Oecologia*, **141**, 191–193.

Shaw MR, Zavaleta ES, Chiariello NR, Cleland EE, Mooney HA, Field CB (2002) Grassland responses to global environmental changes suppressed by elevated CO_2. *Science*, **298**, 1987–1990.

Sherry RA, Weng E, Arnone JA III *et al*. (2008) Lagged effects of experimental warming and doubled precipitation on annual and seasonal aboveground biomass production in a tallgrass prairie. *Global Change Biology*, **14**, 2923–2936.

Sitch S, Huntingford C, Gedney N *et al*. (2008) Evaluation of the terrestrial carbon cycle, future plant geography and climate-carbon cycle feedbacks using five Dynamic Global Vegetation Models (DGVMs). *Global Change Biology*, **14**, 2015–2039.

Smith NG, Malyshev SL, Shevliakova E, Kattge J, Dukes JS (2015) Foliar temperature acclimation reduces simulated carbon sensitivity to climate. *Nature Climate Change*, **6**, 407–411.

Spiegelhalter DJ, Best NG, Carlin BP, van der Linde A (2002) Bayesian measures of model complexity and fit. *Journal of the Royal Statistical Society: Series B (Statistical Methodology)*, **64**, 583–639.

Thornley JH (1976) *Mathematical Models in Plant Physiology*. Academic Press (Inc.) London, Ltd., London.

Walker AP, Hanson PJ, De Kauwe MG *et al*. (2014) Comprehensive ecosystem model-data synthesis using multiple data sets at two temperate forest free-air CO_2 enrichment experiments: model performance at ambient CO_2 concentration. *Journal of Geophysical Research: Biogeosciences*, **119**, 937–964.

Waring R, Landsberg J, Williams M (1998) Net primary production of forests: a constant fraction of gross primary production? *Tree Physiology*, **18**, 129–134.

Webb NP, Stokes CJ, Scanlan JC (2012) Interacting effects of vegetation, soils and management on the sensitivity of Australian savanna rangelands to climate change. *Climatic Change*, **112**, 925–943.

Williams M, Rastetter E, Fernandes D *et al*. (1996) Modelling the soil-plant-atmosphere continuum in a Quercus-Acer stand at Harvard Forest: the regulation of stomatal conductance by light, nitrogen and soil/plant hydraulic properties. *Plant, Cell & Environment*, **19**, 911–927.

Williams M, Schwarz PA, Law BE, Irvine J, Kurpius MR (2005) An improved analysis of forest carbon dynamics using data assimilation. *Global Change Biology*, **11**, 89–105.

Wittig VE, Bernacchi CJ, Zhu XG *et al*. (2005) Gross primary production is stimulated for three populus species grown under free-air CO_2 enrichment from planting through canopy closure. *Global Change Biology*, **11**, 644–656.

Zaehle S, Medlyn BE, De Kauwe MG *et al*. (2014) Evaluation of 11 terrestrial carbon–nitrogen cycle models against observations from two temperate free-air CO_2 enrichment studies. *New Phytologist*, **202**, 803–822.

Zelikova TJ, Williams DG, Hoenigman R, Blumenthal DM, Morgan JA, Pendall E (2015) Seasonality of soil moisture mediates responses of ecosystem phenology to elevated CO_2 and warming in a semi-arid grassland. *Journal of Ecology*, **103**, 1119–1130.

Supporting Information

Additional Supporting Information may be found in the online version of this article:

Appendix S1. Preliminary analysis for choosing the five-two-way interaction terms.
Appendix S2. Bayesian framework and prior distributions.
Appendix S3. Calculation of the data products and associated uncertainty for Fig. 5.
Appendix S4. Description of the setup for each of the Terrestrial Biosphere Models run at the PHACE site.